

Universal corrections to the entanglement entropy in gapped quantum spin chains: A numerical study

Emanuele Levi,¹ Olalla A. Castro-Alvaredo,¹ and Benjamin Doyon²¹*Department of Mathematics, City University London, Northampton Square, London EC1V 0HB, United Kingdom*²*Department of Mathematics, King's College London, Strand, London WC2R 2LS, United Kingdom*

(Received 8 May 2013; revised manuscript received 26 August 2013; published 30 September 2013)

We carry out a numerical study of the bipartite entanglement entropy in the gapped regime of two paradigmatic quantum spin chain models: the Ising chain in an external magnetic field and the antiferromagnetic XXZ model. The universal scaling limit of these models is described by the massive Ising field theory and the $SU(2)$ -Thirring (sine-Gordon) model, respectively. We may therefore exploit quantum field theoretical results to predict the behavior of the entropy. We numerically confirm that in the scaling limit, corrections to the saturation of the entropy at large region size are proportional to a modified Bessel function of the first kind, $K_0(2mr)$, where m is a mass scale (the inverse correlation length) and r the length of the region under consideration. The proportionality constant is simply related to the number of particle types in the universal spectrum. This was originally predicted by J. L. Cardy, O. A. Castro-Alvaredo, and B. Doyon [*J. Stat. Phys.* **130**, 129 (2008)] and B. Doyon [*Phys. Rev. Lett.* **102**, 031602 (2009)] for two-dimensional quantum field theories. Away from the universal region our numerics suggest an entropic behavior following quite closely the quantum field theory prediction, except for extra dependencies on the correlation length.

DOI: [10.1103/PhysRevB.88.094439](https://doi.org/10.1103/PhysRevB.88.094439)

PACS number(s): 75.10.Pq, 03.65.Ud, 02.30.Ik, 11.25.Hf

I. INTRODUCTION AND DISCUSSION

Entanglement is a fundamental property of the state of a quantum system. In the context of quantum computation, it is a crucial resource.¹ Conceptually, it characterizes the structure of quantum fluctuations in a more universal way than other widely studied objects such as correlation functions. Developing theoretical measures of entanglement is therefore important to further understand the structure of quantum states, a problem of particular interest and difficulty for quantum many-body systems. A popular measure of entanglement is the bipartite entanglement entropy. It measures the entanglement between two complementary sets of observables in a quantum system.² Interestingly, the entanglement entropy exhibits universal behavior near quantum critical points: It has features which do not depend on the details of the model but rather on its universality class. In the last decade, this property has made the study of the entanglement entropy a very active field of research.

A fertile testing ground for these ideas is the study of quantum spin chains. A quantum spin chain is a one-dimensional array of particles with spin degrees of freedom and, for our purposes, with nearest- (or few-nearest-) neighbor interactions (this is a local spin chain). Quantum spin chains have been realized in experiments.³ They provide ideal toy models for the study of a whole range of physical phenomena, as they describe interacting many-body systems yet are simple enough to allow for the computation of many quantities. This is especially true for integrable spin chains, since integrability gives rise to the complete characterization of the energy spectrum and states through techniques such as the coordinate and algebraic Bethe ansatz (see, e.g., Ref. 4). Quantum spin chains are extensively studied in the context of quantum information science⁵ and their bipartite entanglement for blocks of consecutive spins has been investigated in many works (see, e.g., Refs. 6–12) both numerically and analytically. Most of these works concentrate on exact critical points.

At the same time, in 1+1-dimensional quantum field theory (QFT) several universal results have been obtained for the entanglement entropy. Two of these results deserve special attention. First, the logarithmic growth of entanglement as the block size increases in conformal field theory (CFT), which is controlled by the central charge.^{13,14} This behavior has been verified for many critical quantum chains.^{6–9,12} Second, the approach to saturation in massive QFT, which is controlled by the mass spectrum.^{15,16} This has not been observed yet in quantum spin chains.

In the present work we investigate the entanglement entropy in two paradigmatic spin chain models (the Ising model and the XXZ model) *near to*, but not at, criticality. We numerically analyze for the first time the universal behavior of the entanglement entropy of a block of length L in the *near-critical scaling limit*. This scaling limit is expected to be described by *massive* QFT. In particular, we confirm massive QFT predictions.^{15,16}

The entanglement entropy is the von Neumann entropy of the reduced density matrix of a state $|\Psi\rangle$ with respect to a tensor factor of the Hilbert space $\mathcal{H} = \mathcal{A} \otimes \mathcal{B}$:

$$S = -\text{Tr}_{\mathcal{A}}(\rho_{\mathcal{A}} \log \rho_{\mathcal{A}}) \quad \text{with} \quad \rho_{\mathcal{A}} = \text{Tr}_{\mathcal{B}}|\Psi\rangle\langle\Psi|. \quad (1)$$

Let $|\Psi\rangle$ be the ground state of a quantum spin chain. In general, it is expected that, thanks to locality, the entanglement entropy of a continuous block A of length L saturates as $L \rightarrow \infty$: It only receives contributions from entanglement between spins surrounding boundary points of A . But this is not so at second-order phase transitions. Assume that the Hamiltonian is parameterized by h , and that there exists a value h_c corresponding to a quantum second-order phase transition (critical point). These critical points are particularly interesting, as they characterize collective quantum behaviors. At $h = h_c$, and in the thermodynamic limit $N \rightarrow \infty$, the correlation length ξ of the ground state is infinite, and the gap $\propto \xi^{-1}$ between the ground state and the continuum of

excited states vanishes: The system is critical. If the dynamical exponent is $z = 1$ (so that the dispersion relation is linear), then the macroscopic, low-energy properties are universal and described by a CFT.

For a block A of length L , the entanglement entropy S diverges for large L as:^{13,14}

$$S(L) \sim \frac{c}{3} \log\left(\frac{L}{\epsilon}\right) + c_2, \quad (2)$$

where c is the central charge of the CFT, ϵ is a short-distance scale (here and below taken as the intersite spacing), and c_2 is a nonuniversal constant. The divergence occurs because with $\xi = \infty$ sites far apart are entangled. Thus we may extract the value of the central charge by studying the divergence of the entanglement entropy in critical spin chains.

In obtaining (2), the order of limits, first $h \rightarrow h_c$ then $L \gg \epsilon$, is very important. Instead, let us take $h \rightarrow h_c$ and $L \gg \epsilon$ “simultaneously”: with $L/\xi =: mr$ fixed. This is the near-critical scaling limit. It is universal, described by a massive QFT corresponding to a perturbation off the original critical point. The mass scale m may be identified with ξ^{-1} . In this limit, the gap of the spin chain is infinitesimally small as compared to microscopic energies (like the intersite interaction energy), but the observation length is so large as to probe only the low-energy, universal, collective excitations of the quantum chain just above the gap; hence the gap still has an effect. The entanglement entropy then has the form of a “saturation term” $(c/3) \log(\xi/\epsilon) + c_1$ which diverges in the scaling limit, where c_1 is another nonuniversal constant, plus a universal scaling function $f(mr)$. The approach to saturation as $mr \rightarrow \infty$ is given by an exponential decay of $f(mr)$ which is solely determined by the spectrum of masses $\{m_i\}$ of the QFT:^{15,16}

$$S = \frac{c}{3} \log\left(\frac{\xi}{\epsilon}\right) + c_1 - \frac{1}{8} \sum_i K_0(2rm_i) + O(e^{-3rm}), \quad (3)$$

where $m \equiv m_1$ is the mass of the lightest particle. Here $K_0(z)$ is the modified Bessel function. Thus, in the near-critical scaling limit, the entanglement entropy of the chain encapsulates information about the mass spectrum of the QFT. Further, despite the nonuniversality of c_1 and c_2 , their difference is universal:

$$U := c_1 - c_2. \quad (4)$$

In massive QFT, U is related to the expectation value of a branch point twist field, as described in Ref. 15. In contrast to the large number of works dealing with critical spin chains, the absence of studies of the near-critical scaling regime precludes a comparison with massive QFT results. The present work intends to fill this gap.

II. ISING MODEL

This model has Hamiltonian

$$H = -\frac{J}{2} \sum_{i=1}^N (\sigma_i^x \sigma_{i+1}^x + h \sigma_i^z), \quad (5)$$

where σ_i^a are Pauli matrices acting on site i and we consider periodic boundary conditions $\sigma_{i+N} \equiv \sigma_i$. $J > 0$ is a “micro-

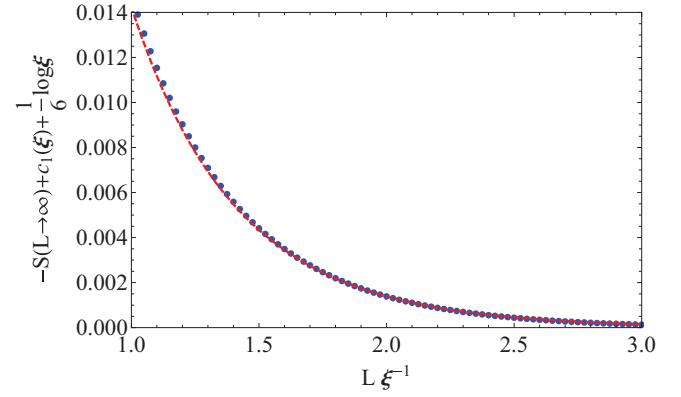


FIG. 1. (Color online) Correction to the saturation of the entanglement entropy of the gapped Ising chain for $\xi = 40$. The solid circles represent the numerical values after subtraction of the exact saturation terms. The dashed red line represents the function $\frac{1}{8} K_0(2L\xi^{-1})$. The agreement is striking and clearly improves for increasing values of $L\xi^{-1}$.

scopic” energy scale, and h plays the role of an external magnetic field. It is well known (see, e.g., Ref. 17) that this model has a quantum critical point for $h = h_c = 1$ described by a CFT with $c = \frac{1}{2}$. The exact correlation length of the chain is given by $\xi^{-1} = \log h$ (Ref. 18) and, as expected, diverges at the critical point. For $h > 1$ the system is gapped and the ground state is unique (no symmetry is broken). Taking the scaling limit described above, a massive QFT is obtained: the free massive relativistic Majorana fermion.

A numerical study of the Ising model has the advantage that a free fermion map can be used to perform computations in the thermodynamic regime. This technique is explained in much detail in Ref. 7 and is based on the use of Toeplitz determinants.⁹ In Appendix A we report a summary of this method, alongside a simple implementation. We can then carry out extremely precise numerics on an exactly infinite chain for very large values of L and very small values of ξ^{-1} .

A numerical computation at the conformal critical point yields the expected behavior (2). For the Ising model, the exact value of $U = -0.131984\dots$ was first evaluated in Ref. 15. With $c_1 = \log 2/2$ calculated in Ref. 19 this gave, using (4), the constant $c_2 = 0.478558\dots$. This agrees extremely well with the numerical results obtained in Ref. 7 and with our own numerics. At the critical point $h = 1$, we find that the entropy is very well described by the function (2) with $c = 0.500003$ and $c_2 = 0.478551$.

Away from criticality the spectrum of the QFT has a single particle. Hence formula (3), with only one term in the sum, should describe the large- mr behavior in the limit $h \rightarrow 1^+$. In our numerics, we take finite, increasing values of ξ , and each time fit the large- L behavior to

$$S = \frac{1}{6} \log \xi + c_1(\xi) - \frac{1}{\alpha(\xi)} K_0(2L/\xi) \quad (6)$$

(we choose $\epsilon = 1$ and use $mr = \frac{L}{\xi}$). We expect $c_1(\infty) = c_1$ and $\alpha(\infty) = 8$. Figure 1 provides an example of such a fit with $\xi = 40$, showing excellent agreement between numerical results and the Bessel function form of the correction to saturation. Figure 2 shows the data for $c_1(\xi)$. The points

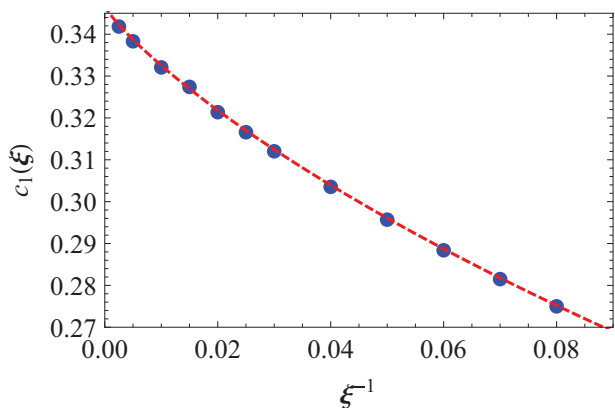


FIG. 2. (Color online) The circles are numerical values of $c_1(\xi)$ obtained by fitting (6). The dashed line represents exactly twice the function in Eq. (13) of Ref. 19, as expected since Peschel's work considers a partition into two semi-infinite regions. The agreement is again extremely good.

agree very well with the exact function of ξ predicted in Refs. 14 and 19 lending support to our method. Finally, Fig. 3 illustrates the main result for the Ising chain. We show the function $\alpha(\xi) =: \alpha_x(\xi)$ obtained from a fit of (6) in regions $L > x\xi$ for $x = 1.5, 2, 2.5, 3, 3.5, 4$, and 4.5 . In all cases, $\alpha_x(\xi)$ appears constant as a function of ξ , and as x increases this constant approaches $\alpha(\infty) = 8$.

III. XXZ SPIN-1/2 MODEL IN THE GAPPED REGIME

Let us now consider the Hamiltonian (with $J > 0$)

$$H = J \sum_{i=1}^N (\sigma_i^x \sigma_{i+1}^x + \sigma_i^y \sigma_{i+1}^y + \Delta \sigma_i^z \sigma_{i+1}^z), \quad (7)$$

with periodic boundary conditions. This is the antiferromagnetic spin- $\frac{1}{2}$ XXZ chain (anisotropic Heisenberg model). This model displays a rich variety of features, depending on the value of the anisotropy parameter Δ . For $\Delta \in (-1, 1]$ the thermodynamic limit $N \rightarrow \infty$ is well described by a CFT with

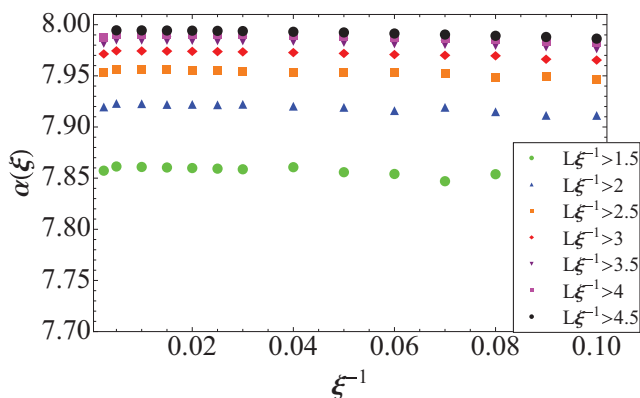


FIG. 3. (Color online) Numerical values of $\alpha_x(\xi)$. Linear fittings of the seven sets of data provide the asymptotic values $\alpha_{1.5}(\infty) = 7.85581$, $\alpha_2(\infty) = 7.9186$, $\alpha_{2.5}(\infty) = 7.95252$, $\alpha_3(\infty) = 7.97121$, $\alpha_{3.5}(\infty) = 7.9818$, $\alpha_4(\infty) = 7.98783$, and $\alpha_{4.5}(\infty) = 7.99146$. Extrapolating in x gives the prediction $\lim_{x \rightarrow \infty} \alpha_x(\infty) = 7.99281$.

$c = 1$ (a free massless boson). For $\Delta > 1$ the model is gapped; hence the scaling limit should be described by a massive QFT. The QFT is the $SU(2)$ -Thirring model (the sine-Gordon model at a special value of its coupling constant—different values of the coupling are recovered by approaching the critical line in other ways; see, e.g., Refs. 20 and 21). This model has a spectrum of two asymptotic particles of equal mass.

In the XXZ model the exact correlation length is given by $\xi(\Delta)^{-1} = \frac{\gamma}{2} + \sum_{n=1}^{\infty} \frac{(-1)^n}{n} \tanh(n\gamma)$, where $\gamma = \cosh^{-1}(\Delta)$.¹⁸

Numerical simulations on the XXZ chain were obtained by employing the density matrix renormalization group (DMRG) approach.²³ In contrast to the Ising example, a new set of technical challenges arises. Whereas in the Ising model we could use formulas for the entropy where the length of the chain was infinity from the outset, in the XXZ case we have to deal with finite chains. This means that if we want to get meaningful results in the scaling limit we need to ensure that $N \gg L$ and, at the same time, if we want to test the behavior (3) we have to consider $L \gg \xi$ while $\xi \gg \epsilon$ is sufficiently large so as to be close to the critical point $\Delta = 1$.

We have found that for a given Δ an optimal choice is achieved by setting $N = 5\xi$. Longer chains are too hard to simulate while for shorter chains boundary effects make it impossible to obtain meaningful results. We considered the cases $\xi = 12, 14, 16, 18, 20$, and 22 , and used again the form (6). We fitted over the range $\xi < L < 2\xi$.

A further challenge is posed by the fact that we have to consider periodic boundary conditions to recover the behavior (6). This makes the convergence of our DMRG algorithm much slower, forcing us to consider up to 1000 states to observe good convergence.

In order to guarantee the correct identification of the ground state we have employed two control parameters: the local magnetization $\langle \sigma_i^z \rangle$ and the truncation error. We used the condition $\langle \sigma_i^z \rangle = 0$ as guiding principle for selecting the ground state. Imposing this condition is quite challenging for periodic chains. In our work we have been able to guarantee $\langle \sigma_i^z \rangle < 10^{-2}$.

For $L \gg \xi$ we observe small oscillations in the entropy between blocks with odd and even numbers of sites. These oscillations are slightly visible in the coefficient $c_1(\xi)$, Fig. 4, and the Bessel function, Fig. 5, and clearly visible in the function $\alpha(\xi)$, Fig. 6. Oscillations in the entropy have been seen for finite chains (see, e.g., Ref. 25) where they arise as a consequence of finite size effects, albeit not for the von Neumann entropy. Clearly, in our case these oscillations must have a different origin. We believe that they are a consequence of the degeneracy of the ground state: For $\Delta > 1$ the ground state is twofold degenerate^{18,24} in the thermodynamic limit (diagonalizing the momentum, two eigenvalues 0 and π occur). Since we are always dealing with finite chains we should never see this degeneracy in our numerical simulations (the state with momentum eigenvalue 0 is the “true” ground state). However for long chains, the gap between the two states narrows and the precision of our algorithm fails to distinguish the energies of those states. The oscillations should then be due to an alternate targeting of two linear combinations of the true (0-momentum) ground state and the π -momentum state (with small amplitude), depending on the parity of L . In Appendix B

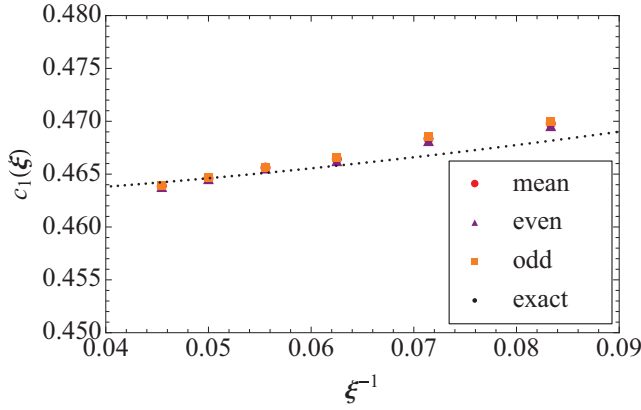


FIG. 4. (Color online) The function $c_1(\xi)$ near the critical point. The points represent the numerical results; the dotted line, the exact function as predicted in Refs. 21 and 22. Denoting by $\tilde{U}(\xi)$ the function (14) of Ref. 21 minus the leading logarithmic term $\frac{1}{6} \log \xi$, the dotted line above is the function $c_1(\xi) = 2\tilde{U}(\xi) + \log 2$. The factor 2 is due to the presence of two boundary points. The term $\log 2$ is related to the degeneracy: Our zero-momentum ground state is composed in equal parts of two Néel-like orthogonal states of the same entropy. This function has the property $c_1(\infty) = 2 \log 2/3$.

we report some details on the simulation parameters, and an explanation of the oscillation phenomenon.

Figure 6 shows that the coefficient $\alpha(\xi)$ converges with great precision to its theoretical value 4. Contrary to the Ising case, $\alpha(\xi)$ has a dependence on the correlation length. Figure 5 shows a good fit to a Bessel function which continues to be good away from $\Delta = 1$ as long as the coefficient $\alpha(\xi)$ is changed as dictated by Fig. 6. Thus the function (6) may provide to a good accuracy a universal description of the entropy of gapped spin chains.

Finally, at the critical point, we have found that the entropy is very well fitted by the function (2) with $c = 1.00024$ and $c_2 = 0.733758$. We can therefore make a prediction for the universal QFT constant $U = c_1(\infty) - c_2 = -0.27166$ in the $SU(2)$ -Thirring model.

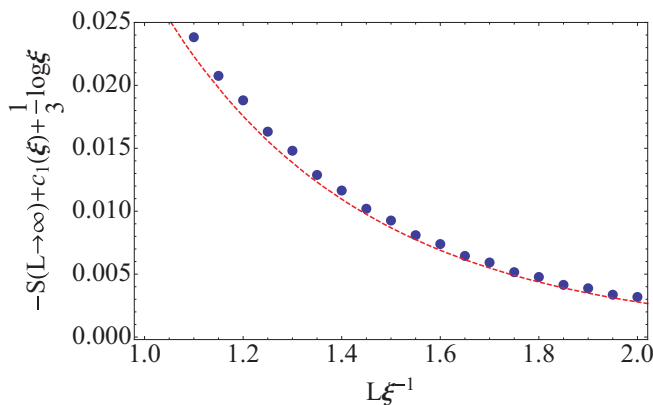


FIG. 5. (Color online) Correction to the saturation of the entanglement entropy of the gapped XXZ chain for $\xi = 20$. The solid circles represent the numerical values after subtraction of the exact saturation terms. The dashed red line represents the function $\frac{1}{4} K_0(2L\xi^{-1})$. The agreement is good and clearly improves for increasing values of $L\xi^{-1}$.

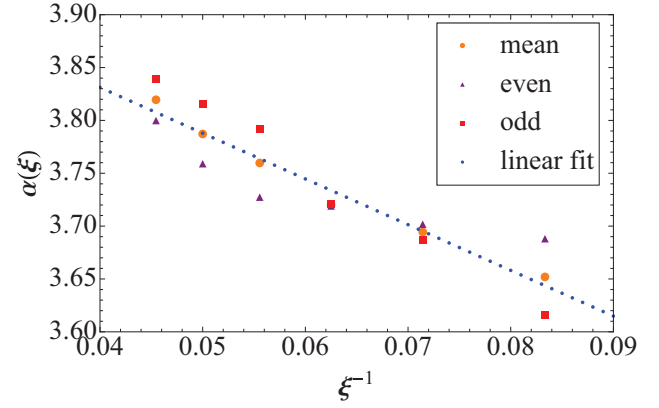


FIG. 6. (Color online) Values of $\alpha(\xi)$ approaching the critical point. The linear expression $\alpha(\xi) = -4.3261\xi^{-1} + 4.0039$ reasonably fits the points and its extrapolation gives $\alpha(\infty) = 4.0039$, which is quite close to the QFT prediction $\alpha^{\text{QFT}} = 4$.

IV. CONCLUSIONS

By studying gapped spin chains we have provided strong numerical evidence for the behavior (3) suggested in Refs. 15 and 16 for two-dimensional QFT. Besides confirming QFT predictions, our results show that computing the entanglement entropy may be a good numerical way to determine the number of lightest particles in the universal spectrum, especially in combination with the knowledge that $\alpha(\infty)$ in (6) must be a fraction of 8. Our results also suggest that some of the QFT predictions may still hold, with small changes, beyond the scaling regime. It would be very interesting to derive this, or the appropriate modification of (6), for spin chains from first principles. We have made a prediction for the universal constant U in the $SU(2)$ -Thirring model, still to be confirmed by means of QFT techniques.

ACKNOWLEDGMENTS

In our study of the XXZ model we have used the numerical recipes provided by ALPS.²⁶ E. L. wishes to thank M. Troyer and A. Feiguin from the ALPS team for their invaluable advice.

APPENDIX A

In this section we report a summary on how to reduce the density matrix of a block of L spins of the ground state $|\Psi\rangle$ of the Ising spin chain into the density matrix of a set of noninteracting free Majorana fermions. This method was first proposed and employed in Refs. 6 and 7. We focus on a chain in its thermodynamic limit, so that it enjoys of translation invariance, and we can take the block made of spins from 1 to L . Our aim is to compute the reduced density matrix $\rho_L = \text{Tr}_{\setminus L} |\Psi\rangle\langle\Psi|$. This is a Hermitian matrix, and its action on the generic spin i can be written as $\alpha_\mu \sigma_i^\mu$, where $\alpha_\mu = (\alpha_0, \alpha_1, \alpha_2, \alpha_3)$ is real, while $\sigma_i^\mu = (\mathbb{1}, \sigma_i^x, \sigma_i^y, \sigma_i^z)$. Then the density matrix takes the form

$$\rho_L = \frac{1}{2^L} \sum_{\mu_1, \dots, \mu_L=0,1,2,3} \alpha_{\mu_1 \dots \mu_L} \sigma_1^{\mu_1} \otimes \dots \otimes \sigma_L^{\mu_L}, \quad (\text{A1})$$

function

```

1  CorrToEntropy[L_] :=
2  Block[{MM, MMM, MMMM, l1, l2, gg, E, Eigen,
3  H},
4
5  MM = Table[0, {i, 1, 2*L}, {j, 1, 2*L}];
6  Do[MMM[j] =
7  ArrayFlatten[Transpose[Table[G[i], {i,
8  0, L - j}]]], {j, 1, L}];
9  Do[Do[MM[[i, j]] = MMM[Ceiling[i/2]][Mod[i
10 + 1, 2] + 1, j - 2*Ceiling[i/2] + 2]],
11 {j, 2*Ceiling[i/2] - 1, 2*L}], {i, 1,
12 2*L}];
13 Do[Do[MM[[j, i]] = -MM[[i, j]], {i, 1,
14 2*Ceiling[j/2] - 2}], {j, 3, 2*L}];
15
16 Eigen = Eigenvalues[MM];
17
18 l1 = Select[Im[Eigen], # > 0 &];
19 l2 = Table[{(l1[[i]] + 1)/2, {i, 1,
20 Length[l1]}}];
21
22 H[x_] := If[Abs[x] > 10^-22 && Abs[1 - x] >
23 10^-22, -x*Log[x] - (1 - x) Log[1 - x],
24 0];
25 E = Chop[Re[Sum[H[l2[[i]]], {i, 1,
26 Length[l2]}]]];
27
28 Return[Re[E]];
29 ];

```

Here the matrix Γ^a defined in (A3) is built in lines 5–8, and then its eigenvalues are stored in the vector `Eigen` in line 10. This vector is used to define the quantities $(1 + v_j)/2$ in lines 12–13, which will be used by the binary entropy H defined in line 15. All this quantities are combined together to compute the block entanglement entropy in line 16.

APPENDIX B

The XXZ model cannot be mapped on a free fermion problem; hence we are not able to use the methods employed for the Ising spin chain. We use the density matrix renormalization group (DMRG) to carry out our simulations. This method has the digitalization of the block density matrix built in, and allows to reach a relatively large block length. This algorithm is based on a truncation in the Hilbert space instead of the high-energy modes of the momentum-space RAG, or the small distance correlations of the real-space RAG. A complete description of the DMRG would be lengthy and out of the scope of this paper; hence we will directly summarize the key steps of our simulation.

(1) We start with the infinite algorithm,²³ until we reach the desired length. We are interested in the scaling properties of the block entropy when the length of the block is from comparable to much bigger than the correlation length. We need then to grow our block far beyond the correlation length.

(2) We perform then the finite algorithm. We take a number of sweeps and states which ensures convergence, and we use the entropy of the final sweep for increasing (e.g., left) blocks to obtain our results. The setting we want to reproduce is the one of a finite block, plugged in an infinite chain, so that we are forced to consider periodic boundary conditions. DMRG's precision relies heavily on the decaying of the entanglement spectrum, which is much slower for periodic boundaries than

TABLE I. In this table the details of our DMRG simulations are reported. N is the length of the chain, m_i the number of states kept in the infinite phase, m_f the number of states kept in the finite phase, and finally ϵ is the truncation error.

Δ	1.92833	1.85021	1.79041	1.74286	1.70394	1.67137
N	60	70	80	90	100	110
m_i	600	600	800	800	800	1000
m_f	600	600	600	800	800	1000
n	60	60	10	80	80	100
$\epsilon(10^{-11})$	1.3	3.4	6.5	3.7	6.2	3.06
$ \langle \sigma_i^z \rangle $	0.0089	0.0068	0.0011	0.01	0.01	0.009

open ones. This forces us to keep more states, and sweep more before observing a good convergence. Good convergence is characterized by a low truncation error, and a symmetric behavior of the entanglement entropy for growing left/right blocks.

We used conserved quantum numbers to speed up the computation. In fact we know that the XXZ Hamiltonian conserves the global magnetization along the anisotropy axis, that is S_z . Moreover we know the ground state has $\langle S_z \rangle = 0$, so that we can focus on that sector.

We considered various values of the anisotropy parameter Δ , corresponding to correlation lengths $\xi = 12, 14, 16, 18, 20$, and 22. In our study the left block must grow much longer than the correlation length in the finite algorithm phase. Clearly longer chains are harder to simulate, and results are less precise. We choose to consider a chain long five times the correlation length as it allows us to obtain good insight on the scaling region, as well as reliable results.

A major problem that arose in performing DMRG simulations on long chains in this regime is the presence of oscillations in the local magnetization and the entropy. In the thermodynamic limit the ground state is twofold degenerate for $\Delta > 1$, as there are two lowest energy states, with different momentum 0 and π ,²⁴ which we call respectively $|\psi_0\rangle$ and $|\psi_\pi\rangle$. This degeneracy is removed in the case of finite periodic chains, where the ground state has zero momentum, while the lowest energy state of the momentum π sector is an excited state. We will refer to these two states again as $|\psi_0\rangle$ and $|\psi_\pi\rangle$ with an abuse of notation. The gap between these two states though becomes very narrow for chains of the length we are considering. At the precision we are working our DMRG algorithm struggles to distinguish these two states. A source of error could be the employment of the Lanczos algorithm for sparse digitalization, which has difficulties in resolving degeneracies. As a result we observe a small staggered behavior for the local magnetization, and a small oscillation in the block entropy between even/odd lengths of the block. Even if $\langle \psi_0 | \sigma_i^z | \psi_0 \rangle = \langle \psi_\pi | \sigma_i^z | \psi_\pi \rangle = 0$, a confusion between these two states can end up giving as target state a superposition $|\Psi\rangle = \alpha|\psi_0\rangle + \beta|\psi_\pi\rangle$, and as a result $\langle \Psi | \sigma_i^z | \Psi \rangle \neq 0$ in general. We use as signal of a good convergence σ_i^z , which we want to be as low as possible.

We used different implementation of the DMRG, but the most precise and reliable results were obtained with ALPS.²⁶ We report in Table I the details of our simulations and results of the convergence tests.

- ¹D. Aharonov, *Quantum Computation*, Annual Reviews of Computational Physics, edited by Dietrich Stauffer, Vol. 6 (World Scientific, Singapore, 1998).
- ²C. H. Bennett, H. J. Bernstein, S. Popescu, and B. Schumacher, *Phys. Rev. A* **53**, 2046 (1996).
- ³J. P. Goff, D. A. Tennant, and S. E. Nagler, *Phys. Rev. B* **52**, 15992 (1995); K. Totsuka, *ibid.* **57**, 3454 (1998); B. C. Watson, V. N. Kotov, M. W. Meisel, D. W. Hall, G. E. Granroth, W. T. Montfrooij, S. E. Nagler, D. A. Jensen, R. Backov, M. A. Petruska, G. E. Fanucci, and D. R. Talham, *Phys. Rev. Lett.* **86**, 5168 (2001); B. Thielemann, Ch. Rüegg, H. M. Rønnow, A. M. Läuchli, J.-S. Caux, B. Normand, D. Biner, K. W. Krämer, H.-U. Güdel, J. Stahn, K. Habicht, K. Kiefer, M. Boehm, D. F. McMorrow, and J. Mesot, *ibid.* **102**, 107204 (2009); A. B. Kuklov and B. V. Svistunov, *ibid.* **90**, 100401 (2003); L.-M. Duan, E. Demler, and M. D. Lukin, *ibid.* **91**, 090402 (2003); J. J. García-Ripoll and J. I. Cirac, *New J. Phys.* **5**, 76 (2003); M. Lewenstein, A. Sanpera, V. Ahufinger, B. Damski, A. Sen(De), and U. Send, *Adv. Phys.* **56**, 243 (2007); Y.-A. Chen, S. Nascimbène, M. Aidelsburger, M. Atala, S. Trotzky, and I. Bloch, *Phys. Rev. Lett.* **107**, 210405 (2011).
- ⁴L. D. Faddeev, Les Houches **1995**, 149 (1996); V. Korepin, N. Bogoliugov, and A. Izergin, *Quantum Inverse Scattering Method and Correlation Functions* (Cambridge University Press, Cambridge, 1993).
- ⁵A. Bayat, S. Bose, P. Sodano, and H. Johannesson, *Phys. Rev. Lett.* **109**, 066403 (2012); A. Bayat, P. Sodano, and S. Bose, *Quant. Inf. Proc.* **11**, 89 (2012); A. Bayat, L. Banchi, S. Bose, and P. Verrucchi, *Phys. Rev. A* **83**, 062328 (2011).
- ⁶G. Vidal, J. I. Latorre, E. Rico, and A. Kitaev, *Phys. Rev. Lett.* **90**, 227902 (2003).
- ⁷J. I. Latorre, E. Rico, and G. Vidal, *Quant. Inf. Comput.* **4**, 48 (2004).
- ⁸J. I. Latorre, C. A. Lutken, E. Rico, and G. Vidal, *Phys. Rev. A* **71**, 034301 (2005).
- ⁹B.-Q. Jin and V. Korepin, *J. Stat. Phys.* **116**, 79 (2004).
- ¹⁰N. Lambert, C. Emary, and T. Brandes, *Phys. Rev. Lett.* **92**, 073602 (2004).
- ¹¹J. P. Keating and F. Mezzadri, *Phys. Rev. Lett.* **94**, 050501 (2005).
- ¹²R. Weston, *J. Stat. Mech.* (2006) L03002.
- ¹³C. Holzhey, F. Larsen, and F. Wilczek, *Nucl. Phys. B* **424**, 443467 (1994).
- ¹⁴P. Calabrese and J. L. Cardy, *J. Stat. Mech.* (2004) P06002; (2005) P04010.
- ¹⁵J. L. Cardy, O. A. Castro-Alvaredo, and B. Doyon, *J. Stat. Phys.* **130**, 129 (2008).
- ¹⁶B. Doyon, *Phys. Rev. Lett.* **102**, 031602 (2009).
- ¹⁷A. O. Gogolin, A. A. Nersesyan, and A. M. Tsvelik, *Bosonization and Strongly Correlated Systems* (Cambridge University Press, Cambridge, 1998); S. Sachdev, *Quantum Phase Transitions*, 2nd ed. (Cambridge University Press, Cambridge, 2011).
- ¹⁸R. J. Baxter, *Exactly Solved Models in Statistical Mechanics* (Academic Press, San Diego, 1982).
- ¹⁹I. Peschel, *J. Stat. Mech.* (2004) P12005.
- ²⁰S. Pallua and P. Prester, *Phys. Rev. D* **59**, 125006 (1999).
- ²¹E. Ercolessi, S. Evangelisti, and F. Ravanini, *Phys. Lett. A* **374**, 2101 (2010).
- ²²P. Calabrese, J. Cardy, and I. Peschel, *J. Stat. Mech.* (2010) P09003.
- ²³S. R. White, *Phys. Rev. Lett.* **69**, 2863 (1992); *Phys. Rev. B* **48**, 10345 (1993); U. Schollwöck, *Rev. Mod. Phys.* **77**, 259 (2005).
- ²⁴A. G. Izergin, N. Kitanine, J. M. Maillet, and V. Terras, *Nucl. Phys. B* **554**, 679 (1999).
- ²⁵P. Calabrese, M. Campostrini, F. Essler, and B. Nienhuis, *Phys. Rev. Lett.* **104**, 095701 (2010); M. Fagotti and P. Calabrese, *J. Stat. Mech.* (2011) P01017; J. C. Xavier and F. C. Alcaraz, *Phys. Rev. B* **83**, 214425 (2011).
- ²⁶A. F. Albuquerque, F. Alet, P. Corboza, P. Dayal, A. Feiguin, S. Fuchs, L. Gamper, E. Gull, S. Gürtler, A. Honecker, R. Igarashi, M. Körner, A. Kozhevnikov, A. Läuchli, S. R. Manmana, M. Matsumoto, I. P. McCulloch, F. Michel, R. M. Noack, G. Pawłowski, L. Pollet, T. Pruschke, U. Schollwöck, S. Todo, S. Trebst, M. Troyer, P. Werner, and S. Wessel, *J. Magn. Magn. Mater.* **310**, 1187 (2007); B. Bauer, L. D. Carr, H. G. Evertz, A. Feiguin, J. Freire, S. Fuchs, L. Gamper, J. Gukelberger, E. Gull, S. Guertler, A. Hehn, R. Igarashi, S. V. Isakov, D. Koop, P. N. Ma, P. Mates, H. Matsuo, O. Parcollet, G. Pawłowski, J. D. Picon, L. Pollet, E. Santos, V. W. Scarola, U. Schollwöck, C. Silva, B. Surer, S. Todo, S. Trebst, M. Troyer, M. L. Wall, P. Werner, and S. Wessel, *J. Stat. Mech.* (2011) P05001; M. Troyer, B. Ammon, and E. Heeb, *Lecture Notes in Computer Science* **1505**, 191 (1998).